Journal of Sol-Gel Science and Technology
https://doi.org/10.1007/s10971-024-06476-9

ORIGINAL PAPER

Foeniculum Vulgare leaf extract loaded synthesis of silver nanoparticles in different volume ratios for antimicrobial and antioxidant activities: Comparative study of composition

Eneyew Tilahun Bekele[1] · Fasika Dereje Ambecha[1] · C. R. Ravikumar[2] · Taymour A. Hamdalla[3] · H. C. Ananda Murthy[4,5] · Defaru Negera Duke[1]

Received: 20 April 2024 / Accepted: 27 June 2024

Abstract

The current world is exposed to immense classes of challenges, of which antimicrobial-caused infectious diseases have been ranked the third killer disease due to their high resistance capability. Oxidative stress is also the other problem faced by the current world. In the current study, a leaf of *Foeniculum Vulgare* was employed for the synthesis of silver nanoparticles (Ag NPs) within the 1:3, 1:1, and 3:1 compositions using 0.1 M of $AgNO_3$. The calculated average crystalline size from X-ray diffraction (XRD) was found to be 12.6, 13.7, and 21.6 nm for the 1:3, 1:1, and 3:1 volume ratios, respectively. Scanning electron microscope coupled with energy dispersive spectroscopy (SEM-EDS) analysis depicts the quasi-spherical shape with an intense Ag peak at around 3.00 eV. Transmission electron microscope coupled with high-resolution transmission microscope with surface area electron diffraction pattern (TEM-HRTEM with SAED) showed spherical shaped Ag NPs. The electronic bandgap energy was calculated as 3.1, 3.2, and 3.3 eV for the 1:1, 3:1, and 1:3 volume compositions, respectively. Ag NPs show 13.5, 12.5, and 11.0 mm zones of inhibition for the 1:3, 1:1, and 3:1 ratios, respectively. The antifungal activity was found to be 16.9, 11.2, and 10.5 mm for the 3:1, 1:3 and 1:1 ratios, respectively. Lastly, the antioxidant activity was estimated to be 42.4, 28.94, and 27.39% RSA for the 1:1, 3:1, and 1:3 volume ratios respectively. All the ratios of Ag NPs showed promised antimicrobial and antioxidant activity in the presence of 2, 2-Diphenyl-1-picrylhydrazyl (DPPH) due to the enhanced generation of reactive oxygen species (ROS).

Graphical Abstract

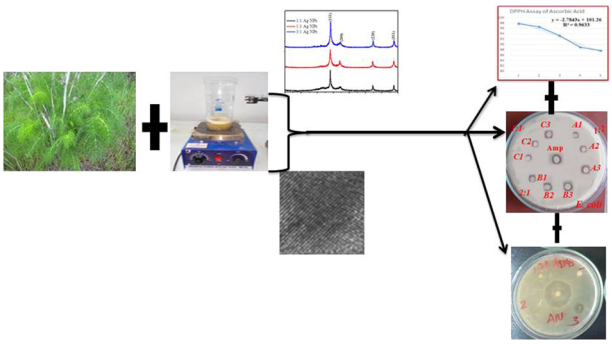

✉ Defaru Negera Duke
defaru.negera.duke@astu.edu.et

[1] Department of Applied Chemistry, School of Applied Natural Science, Adama Science and Technology University, P O Box 1888 Adama, Ethiopia

[2] Research Centre, Department of Science, East-West Institute of Technology, Bangalore 560091, India

[3] Physics department, faculty of science, University of Tabuk, Tabuk, India

[4] Department of Applied Sciences, Papua New Guinea University of Technology, Lae, Morobe Province 411, Papua New Guinea

[5] Department of Prosthodontics, Saveetha Dental College & Hospital, Saveetha Institute of Medical and technical science (SIMAT), Saveetha University, Chennai 600077 Tamil Nadu, India

Published online: 16 August 2024

Keywords Ag nanoparticles · *Foeniculum Vulgare* leaf · antimicrobial and antioxidant

Highlights

- Green Synthesis of Ag NPs within three volume ratios in the presence of *Foeniculum vulgare* leaf extract.
- Investigating the potential antibacterial, antifungal, and antioxidant activities.
- Comparative study of the volume ratios on the antimicrobial and antioxidant activities.

1 Introduction

Currently, antimicrobial infectious disease caused by a variety of sources accounts for the death of millions of people each year, which occurs in the global arena. Microbes such as bacteria and fungi pose an imperative threat to human beings around the globe. Nowadays, these disease-causing pathogens become more resistant to the upcoming commercially available antibiotic drugs. Antimicrobial infectious disease has been a worldwide public health threat and one of the top-killer diseases due to its high resistance to antibiotics. According to a recent report by the Organization of World Health (WHO), infectious diseases related to drug-resistant microbes have a higher rate of death at all ages of human beings [1]. The continual increase of feasting of antimicrobial agents and inappropriate use as well as uncontrolled migration of peoples across the world led to the comprehensive of multidrug-resistant strains. Most importantly, antibiotic-resistant bacteria are a worldwide global problem that has emerged due to the misuse and long-term administration of antibiotics. Bacteria exposed to antibiotics can acquire resistance to antibiotics. Such pathogens transmit resistance to other microorganisms, giving them the same properties. In addition to this, the resistance to one antibiotic may manifest as resistance to many other antibiotics that share the same structure, resulting in multi-drug resistant (MDR) strains [2, 3].

The currently available commercially synthesized antibiotics become unable to treat the infectious diseases caused by various classes of bacteria pathogens. Bacteria-caused infectious diseases have been found to be very serious, specifically in low-income countries, and lead to the death of infants, pregnant, and old people. MDR bacterial infection diseases may lead to an increase in mortality and morbidity rates, prolonged hospitalization periods, and economic loss all over the world. Health centers around the world do not have effective alternatives to treat infected patients due to the development of MDR bacteria and super germs. Thus, in the recent world, researchers have exaggerated the design and development of a new effective antibacterial nano-based drug, which is needed, as there is a growing concern in MDR [4]. As such, nanoparticles, specifically metal NPs such as Ag NPs fabricated via green cost-effective methods have been the potential candidate that would be repairable in preventing and treating both Gram-negative and Gram-positive pathogenic bacteria, which is the current most killer disease in the world. Green synthesized Ag NPs could used to treat immense bacterial-caused infectious diseases such as *E. coli*, *S. aureus*, *P. aeruginosa*, and *S. pyogen*. This is due to its suitable properties and as well as the high generation of ROS contributed from the use of the bioactive ingredients. An exploration of the reduction of Ag NPs is principally contributed to the reducing properties of biomolecules of plants such as flavones, polyphenols also terpenoids. This allows for the formation of stable high surface area Ag NPs with the excessive generation of the ROS radicals, which plays a vital role in slowing down the growth and later the death of the bacterial cell membranes [5]. Green Ag NPs prompt neutralization of the surface charge of bacterial membranes and change its permeability and then leading to the death of bacteria [4, 5].

Furthermore, fungal infections diseases are increasing worldwide due to the presence of various sources of infections. Since the way of prevention of such infections, diseases are mostly combated with the use of antibiotics, which has been nullified by fungi resistance. This might be ascribed due to the retardation in the activity of antifungal drugs that can be lost their usefulness in curing infectious diseases caused by innumerable classes of fungi due to the presence of various side effects and the development of resistance by such fungi species [4]. This has intern solidified the treatment of fungi infections disease a difficult and a major challenge in the world. The extreme practices of antifungal therapy in the health zone have been reported to contribute massively to antibiotic resistance. Fungal-caused diseases not only disturb the health system of human beings but also fatal classes of diseases that affect the world economic system. Fungi species such as *Aspergillus niger* and *Candida albicans* have been the most common pathogens that reduce crop productivity, affects and reduces the production of different types of fruits and vegetables. Due to such fact, the finding of an effective drug against fungal pathogens drug needs the attention of researchers globally. In comparison to the commercially available drugs, green synthesized NPs, most importantly metal NPs such as Ag have been the highly investigated NPs, due to their suitable

physico-chemical and structural properties towards the targeted applications [6].

In addition to its effective antimicrobial activity, green synthesized Ag NPs also possessed potential antioxidant activity (ability of molecules to scavenge free radicals). The oxidative stress resulting from the inequity between fabrication and accumulation of ROS has been another critical health problem around the globe. Oxidative stress is a marvel that can be demarcated as a state when the equilibrium between the antioxidative defense of the cell and oxidants is disrupted by the presence of excessive amounts of oxidants such as reactive oxygen or nitrogen species and organic compounds containing sulfur-producing alkyl sulfanyl radicals ($RS^{\bullet}$) [7]. Oxidative stress has not only negative effects on the human body but also as free radicals have a nonpareil function in living organisms. Along with this, in order to keep and enhance the shelf life of various products, the use of high surface area-based antioxidant material is the pillar secure methodology that enhances the economical pathway. There have been numerous ways of determining the antioxidant capacity of materials, which is based on different methodologies and assays. Recent reports proved that among the different ways, the use of green synthesized NPs, specifically metal oxides such as Ag, is a farfetched potential [8]. Due to this fact, Ag NPs also showed astonishing impending activity in the treatment of degenerative disease. Therefore, exploration of the potent antimicrobial and antioxidant applications of green Ag NPs has now been the ultimate candidate in research and health centers. The plant *Foeniculum vulgare* is a well-known spice and traditional medicine for different diseases such as kidney stones, gonorrhea, fever, sleeplessness, renal problems, laxative, leucorrhoea, nosebleeds, diuretic diaphoretic, liver discomfort, mouth ulcer, and stomachache, belong to the *Umbelliferae family* [9, 10]. Since the plant is a rich source of ketones, flavonoids, protein, fiber, carbohydrates, and vitamins. Due to this fact, it could be also explored as a potential templating agent for the synthesis of Ag NPs.

Foeniculum vulgare is a biennial medicinal plant belonging to the family of Apiaceae [11]. This medicinal plant is well known for having anti-inflammatory, antispasmodic, antiseptic, carminative, diuretic, hypocholestrolaemic, antidiabetic, analgesic, antipyretic, CNS-stimulant, antioxidant, wound healing, and immune-modulatory activity as well as gastro-protective and chemo-preventive activities, analgesic effect and is effective in gastrointestinal disorder treatment [12]. Also with its antiulcer and anti-properties, it is used to treat neurological disorders. Specifically, fresh leaves are also traditionally used to treat, Gonorrhoea, Gland TB (Naqarsa), Kidney disease, and Nosebleeds [13]. In addition, the medicinal plant plays a vital role in the synthesis of stable NPs, used to avoid the use of expensive and toxic capping agents. This is due to the unique future of its bioactive components, which were used to cape and stabilize the shape and size of Ag NPs for the targeted applications. This again enhances the generation of a high amount of ROS, which is an essential factor for the antimicrobial and antioxidant activity of Ag NPs.

Microbial infectious diseases and antioxidant stress become serious health problems that have drawn public attention worldwide as a human health threat that extends to economic and social complications. Since, the most common challenges with microbial infectious diseases and antioxidant stress are not only mortality and morbidity but in terms of treatment costs, low efficiency of treatment, and insufficient distribution to society [14]. Therefore, the design and development of continual solutions for such global problems need immediate solutions. One of the most cost-effective and at the same time efficient for the mentioned problems is the green synthesis of Ag NPs in the presence of medicinal and spices plants as a templating agent. In the previous literature, various techniques of Ag NPs synthesis for immense applications have been documented. However, the fabrication of Ag NPs in the presence of leaf extract of *Foeniculum vulgare* within different volume ratios of extract to precursor salt as antimicrobial and antioxidant activity has not yet been reported. Furthermore, to the best of our knowledge, no study has been reported on the effect of volume ratios on the antibacterial, antifungal, and antioxidant applications elsewhere. The focus of the current report is therefore to investigate the synthesis of Ag NPs loaded *Foeniculum vulgare* leaf within different ratios such as 1:3, 1:1, and 3:1, characterization using different advanced techniques, and to investigate its potential antibacterial, antifungal, and antioxidant applications. Moreover, a comparative analysis of volume ratios on the targeted applications has been well reported. Lastly, the study spectacle the fabrication of stable green Ag-based nano-level drug for the study under consideration.

2 Methodology

2.1 Chemicals and Regents

During the study, different solvents, chemicals, and regents have been used such as DH_2O (AR), silver nitrate ($AgNO_3$, Sigma Aldrich), absolute ethanol (99.9% Lab Tech Chemicals), ethanol reagent (97%), 2, 2-diphenyl-1-picrylhydrazyl (DPPH, AR), Müller-Hinton agar, ampicillin, sodium hydroxide (NaOH) (Sigma-Aldrich), and dimethyl sulfoxide (DMSO, AR). The mentioned chemicals are analytical grades and so used without any auxiliary treatment and cleansing.

Fig. 1 Phytochemical test for alkaloid (i), flavonoid (ii),cannins (iii), terpenoid (iv), steroid (v), glycosides (vi),benedicts (vii), phenol(viii) and saponin (viiii)

2.2 Phytochemical test

The presence/absence of various bioactive molecules within the leaf extract of *Foeniculum vulgare* that was used as a reducing and capping agent during the synthesis of Ag NPs was assessed via phytochemical tests such as saponin, phenols, benedict, glycoside, steroids, terpenoids (Salkowski test, tannins (ferric chloride test), flavonoids, alkaloids (Wagner's test) following previous standard procedures with certain modifications [15]. Figure 1 displays the color change for each of the phytochemical tests of *Foeniculum vulgare* leaf extract.

2.3 Collection and extraction of *Foeniculum vulgare*

Foeniculum vulgare leaf was collected from the agricultural research center of Wondo Genet branch, Sidama Region, Ethiopia. The collected leaf was washed several times with distilled water to remove any surface contaminants and dust particles. Then later, the cleaned leaf was allowed shadow drying at room temperature in the open air for about 15 days to remove any remaining moisture content from the washed leaf. The dried leaf was then grinded using an electrical grinding machine to produce a fine powder of the leaf followed by packing it in a brown bottle by covering it with aluminum foil to protect against the effect of light. The extraction process was done by taking 25 g of the leaf powder followed by the addition of 800 mL of DH_2O at 50 °C for 40 minutes [16]. The crude extract was then cooled to room temperature and filtered. The filtrate was packed within a colored bottle glass followed by covering with aluminum foil. At the end, the packed filtrate stayed in the refrigerator at 4 °C for the synthesis of Ag NPs within different volume ratios.

2.4 *Foeniculum vulgare* leaf templated Synthesis of Ag NPs

Synthesis of Ag NPs has been carried out using 0.1 M of $AgNO_3$ by adapting the previously reported procedure, with minor modifications. Ag NPs were synthesized in three different volume ratios 1:1 (100:100), 1:3 (50:150), and 3:1(150:50) using 0.1 M precursor salt with *Foeniculum vulgare* leaf extract, respectively in a separate reaction medium. A small-sized magnetic bar was put inside the beaker containing the leaf extract and the precursor solution to boost the reaction kinetics in each of the individual ratios. Then the mixtures were heated at 30 °C for 1 h on the hot plate with stirring and after 1 h, the heater was turned off and the mixed components were stirred for an additional 3 h. The suspension later showed a brownish color, which indicates the formation of Ag NPs. After the reaction time was completed, the formed suspensions at different volume ratios were allowed to stay in a refrigerator overnight. Then the drifted components above the formed precipitate were decanted very carefully and the formed precipitate for each of the individual ratios was washed with ethanol and distilled water 3 times by centrifugation for 15 min at 15000 rpm. After the end of the centrifugation, each of the individual ratios was then collected using a crucible ceramic dish and placed into a drying oven at 100 °C. It was then later allowed to cool and the obtained product was ground into a small fine powder [17]. Finally, the gray powder was packed for the next characterization and applications (Fig. 2). This specific experimental synthesis condition method was chosen based on environmental friendliness, in terms of the high generation of ROS content, and then to achieve small-sized Ag NPs.

2.5 Method of antimicrobial activity

2.5.1 Antibacterial activity test

The biosynthesized Ag (1:1, 1:3, and 3:1 ratio) NPs were screened for in-vitro antibacterial activities against Gram-negatives (*E.coli* and *P. aeruginosa*) and Gram-positive (*S. aureus* and *S. Pyogen*) via agar disc diffusion technique. Initially, the medium was prepared by dissolving the 38 g of Mueller Hinton Agar within 1000 mL of distilled water and autoclaved at 121 °C for 15 min. The autoclaved medium was then poured into the sterile plates (20–25 mL/plate) and the plates were allowed to solidify under the sterile

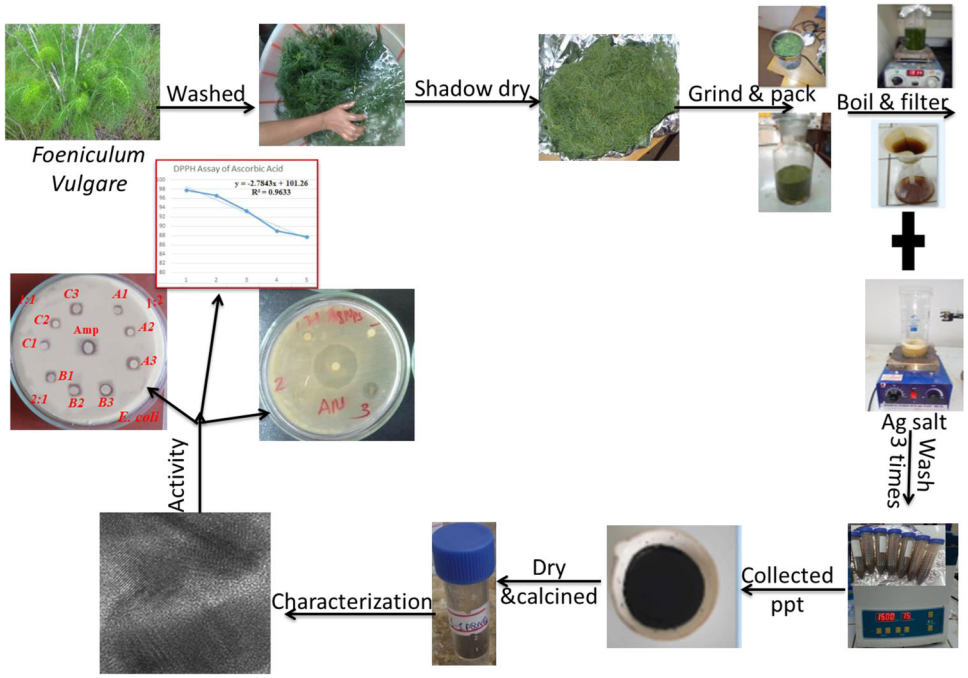

Fig. 2 Displays the schematic graphical synthesis procedure of Ag NPs within a 1:1 volume ratio

condition at room temperature. The plates were then seeded with overnight grown culture approximately 1.5×10^8 CFU/mL (McFarland standard) by swabbing evenly onto the surface of the medium with a sterile cotton swab. Then, 35 mg from each of the three ratios of Ag NPs at the concentrations of 50, 75, and 100 µg/mL per disc was prepared by dissolving within 1 mL of DMSO and stirred for 30 min. From these solutions different concentrations of 50, 75, and, 100 µg/mL were poured using a micropipette in each pathogen well. Whatman filter paper no. 1 was used to prepare discs approximately 6 mm in diameter. From each different ratio, 80 µL aliquots were taken and saturated with discs (6 mm diameter) and positioned on the surface of the medium with sterile forceps and gently pressed down to ensure contact with the MHA. The plates were then inverted and incubated at 37 °C for 24 h. After incubation, the potential activities of Ag NPs were evaluated by measuring the diameter (mm) zone of inhibition around the disc against the test [18].

2.5.2 Antifungal activity test

The antifungal activities of Ag NPs (1: 1, 1: 3, and 3: 1) were tested against *Aspergillus niger* and *Candida albicans* using the disc diffusion method. First, solutions 15, 20, and 25 mg/mL from each volume ratio of Ag NPs were prepared by reconstituting 0.015, 0.020, and 0.025 gm of each Ag NPs powder in 10 mL of DMSO within a separated flask. The required amount of PDA and SDA were dissolved in distilled water. Then the resulting mixture was heated on the hot plate and autoclaved to get a boiled and uniform solution. Solidify the resulting autoclaved medium transferred into the separated petri plates. Within 15 min of adjusting the turbidity of the suspension of inoculums, a sterile cotton swab was dipped into the adjusted suspension and rotated several times by pressing firmly on the inside wall of the tube above the fluid level. Then, the dried surface of PDA and SDA plates was inoculated by streaking using the swab three times over the entire surface by rotating the PDA and SDA plates at approximately 60° to ensure an even distribution of the inoculums. Then, the PDA and SDA plates were left open for 3–5 minutes to allow any excess surface moisture to be absorbed. To investigate the potential antifungal activity of Ag NPs, discs of 6 mm diameter were prepared from sterile filter paper cut into small circular pieces of equal size and then impregnated each with 0.01 mL of the prepared green Ag NPs. The Ag NPs-impregnated discs were placed onto the surface of the inoculated agar plates using sterile forceps. Each disc was pressed down to ensure complete contact with the agar surface. The discs were distributed evenly so that they were no closer than 24 mm from center to center. Discs of commercial Ketoconazole (10 units/disc) were used as positive control while DMSO-impregnated discs were used as negative control. Then the PDA and SDA plates were sealed with Parafilm and incubated at 27 °C for 5–7 days for fungal pathogens [19]. After the incubation period had been completed, the zone of inhibition around each disc was measured to the nearest mm along two axes (i.e. 90° to each other) using a transparent ruler. The experiment was performed in three replications and then means ± SD value for each volume ratio of Ag against the selected fungal pathogen were taken.

Table 1 Qualitative phytochemical analysis of *Foeniculum vulgare* leaf extract

No.	Phytoconstituents	Chemical test/reagent	Results	Observed color
1	Alkaloid	Wagner's test	+	brown/reddish precipitate
2	Flavonoids	Alkaline Reagent Test	+	Yellow
3	Tannins	Ferric Chloride test	+	Brownish-green
4	Terpenoid	Salkowski test	+	reddish-brown
5	Steroid	Salkowski test	+	Red
6	Glycosides	Salkowski test	+	reddish-brown
7	Benedict	Benedict test	+	Blue-green
8	Phenols	Ferric Chloride test	+	Black
9	Saponin	Frothing test	+	Stable persistent froth

2.5.3 Antioxidant activity test

The DPPH assay technique was used to investigate the activity of free radical scavenging for each of the volume ratios of green Ag NPs by measuring the diminution in the absorbance fixed at 517 nm. The stock solution was prepared by taking 8 mg from each of the volume ratios of Ag NPs followed by adding 5 mL of methanol. The serial solution was done to spring 50, 100, 200, 400, and 800 µg/mL in five vials. Then 1 mL from each serial dilution 4 mL DPPH was mixed together and shaken vigorously [18]. The resulting solution was placed in a dark place at 37 °C for 30 minutes and subjected to UV-Vis spectrophotometer to record the resulting absorbance at 517 nm in the presence of ascorbic acid as a standard and dissolved. Finally, the absorbance values were measured and the antioxidant activities were calculated using the following Eq. 1.

$$\%\,\text{of antioxidant acitivity} = \frac{\text{Control OD} - \text{Experimental OD}}{\text{Control OD}} * 100\% \quad (1)$$

Where Control OD = Absorbance of the sample without Ag NPs; Experimental OD = Absorbance of the sample with Ag NPs. The results obtained were expressed as a percentage decrease with respect to the control.

3 Results and discussion

3.1 Phytochemical investigation analysis

The resulting phytochemical analysis of *Foeniculum vulgare* leaf perceived the presence of immense bioactive molecules. Their presence played a vital role as a capping and reducing agent during the synthesis of Ag NPs within different volume ratios. The color change with the "+" confirms the presence of functional groups such as alkaloids, flavonoids, tannins, terpenoids, steroid,s and starch (Table 1) [20, 21].

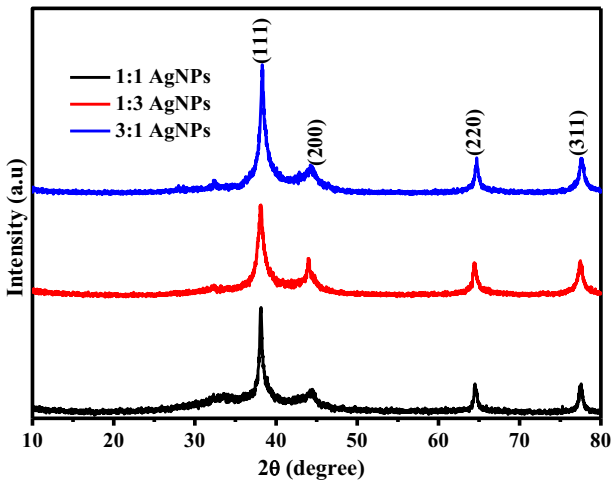

Fig. 3 XRD graph of *Foeniculum vulgare* leaf templated Ag NPs

3.2 XRD Analysis

The X-ray diffraction (XRD-7000, SHIMADZU Corporation, Japan) equipped with a Cu target and $\lambda = 0.15406$ nm was recorded in the range of 10 to 80θ. The XRD analysis was used to evaluate expansively the degree of phase purity, the estimated average crystal size, and details of the crystal structure of green synthesized Ag NPs. As can be depicted in Fig. 3, each of the three-volume ratios of Ag NPs showed peaks at 38.21°, 44.38°, 64.77°, and 77.58° corresponding to the (111), (200), (220), and (311) crystallographic planes, respectively. Each of the ratios of green Ag NPs fitted with the JCPD card number of 00-004-0783. This ascribed that *Foeniculum vulgare* leaf extract templated synthesized Ag NPs is strongly pure without any additional phase formation as impurities. The XRD pattern of Ag NPs showed sharp and intense peaks indicating the finely ground and homogenized with high crystalline quality [22].

The relative average crystalline sizes of green Ag NPs were estimated using the equation Scherer's. The value was obtained as 12.6, 13.7, and 21.6 nm for the 1:3, 1:1, and 3:1

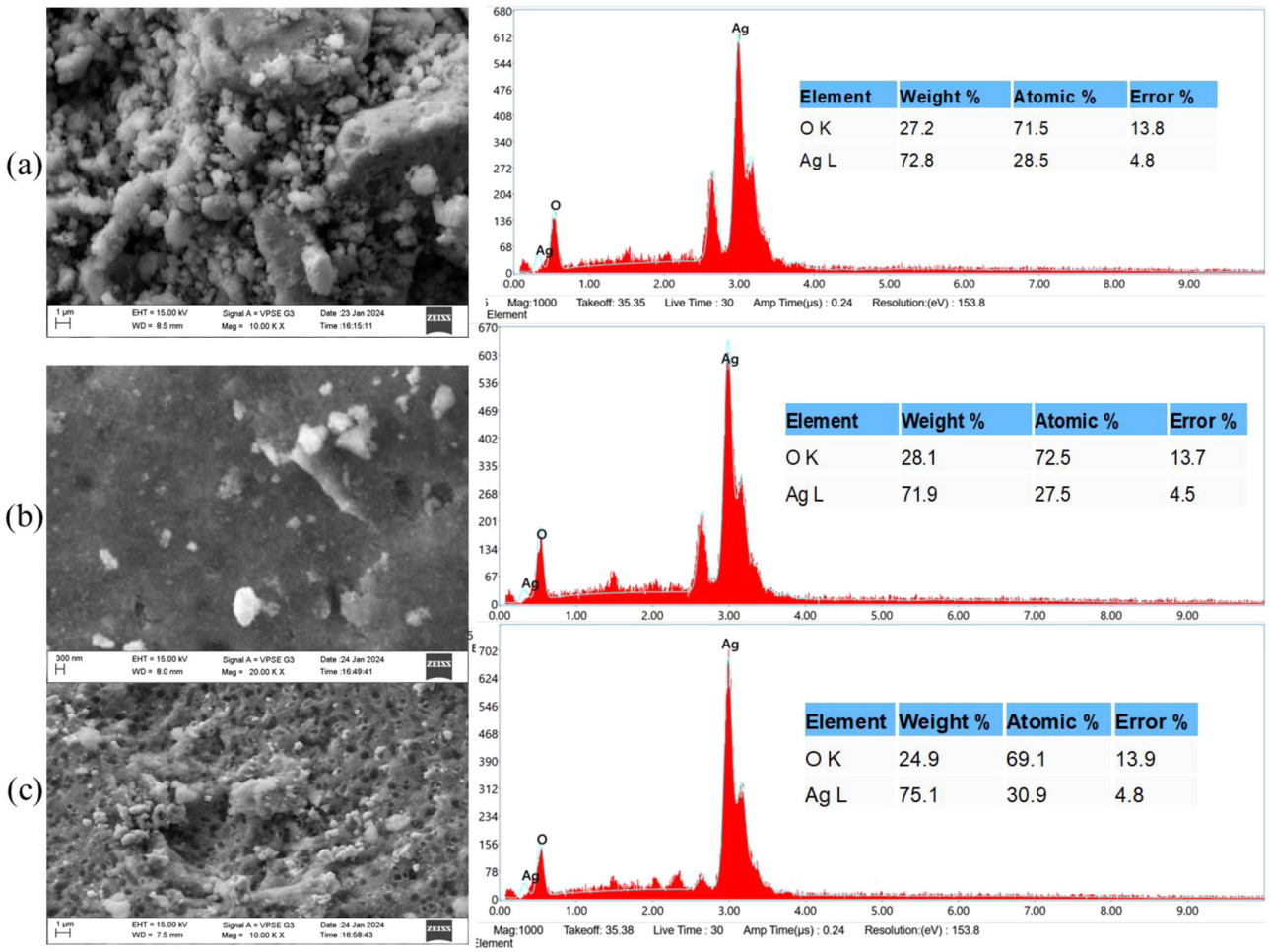

Fig. 4 SEM-EDS image of *Foeniculum vulgare* leaf templated Ag NPs. **a-c** are the SEM images of the 1:3, 1:1, and 3:1 ratios, respectively

volume ratios of precursor to leaf extract, respectively. The alteration in the calculated average crystalline size is due to the change in the volume ratios of extract to precursor salt. As can be ascribed in Fig. 3, Ag (1:3) showed broad and short peak intensity, as compared to the counterpart ratios. This indicates the relatively smaller size of the 1:3 ratios followed by the 1:1 ratios of Ag NPs. The calculated average crystalline directly fits with the peak broadening and intensity. As the amount of the extract to be added is enhanced, a smaller size is achieved. This is because the presence of an excessive amount of extract leads to more reduction and at the same time stabilization of the suspension during the synthesis process. In addition, the availability of more reducing agents leads to higher nucleation rates. This intern increased nucleation rate can result in the formation of a larger number of smaller-sized Ag nuclei. This again leads to the formation of smaller averaged Ag NPs crystalline sizes [17]. However, in opposition, the smaller amount of extract used results in less capping and particle growth is high.

3.3 SEM-EDS analysis

The surface morphology futures and elemental composition of each of the green-formed Ag NPs were analyzed using SEM equipped with EDS (SEM–EDX-EVO 18 model-low vacuum facility-ALTO 1000 Cryo attachment) spectroscopy. Figure 4a–c presents the SEM image of 1:3, 1:1, and 3:1 volume ratios of Ag NPs with their corresponding EDS histogram (on the right).

The surface morphology of each Ag NPs nearly quasi-spherical in the presence of aggregation. The formation of aggregation in some places of the SEM image is a direct confirmation of the use of the extract [23]. In addition, the formation of aggregation might be attributed to the process of dehydration exerted during the sample preparation stage for SEM analysis. Furthermore, Ag (1:3) NPs also showed rod-like structures dominated by the spherical morphology. The SEM image also revealed a high density of Ag NPs in the presence of a quasi-spherical structure. On the other hand, the EDS analysis was employed to detect the

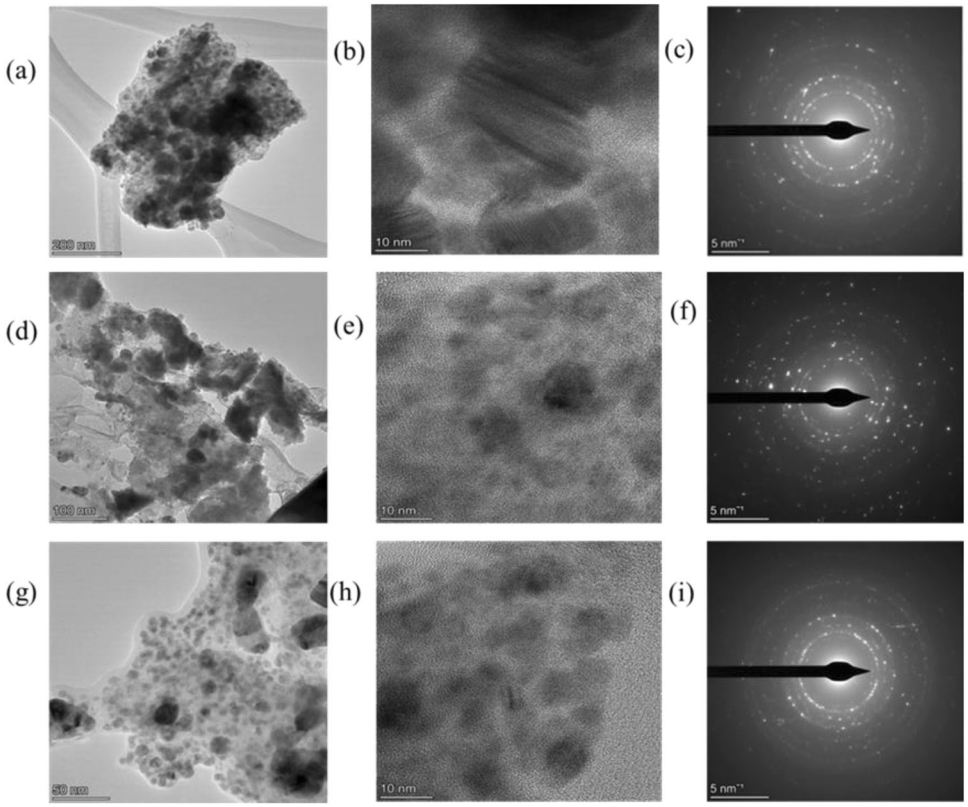

Fig. 5 TEM-HRTEM and SAED pattern of *Foeniculum vulgare* leaf extract supported Ag NPs. **a**-**c** are TEM of 1:3, 1:1, and 3:1, respectively; **d**-**f** are HRTEM of 1:3, 1:1, and 3:1, respectively; **g**-**i** are SAED of 1:3, 1:1, and 3:1, respectively

elemental composition of green Ag NPs. The EDS graph depicted that the synthesized Ag NPs were free of impurities, as also confident from the XRD analysis (00-004-0783). The dominant strong peaks in each of the volume ratios are Ag NPs located around 3.00 eV in the presence of minor peaks of the O atom. The obtained peak values of EDS comply with those reported before [24]. The absence of any spotted peaks in the EDS graph is attributed to the good centrifugation and washing of the Ag samples after the compilation of the reaction [25]. The atmospheric oxygen dominantly contributed to the presence of O in the EDS spectrum of Ag NPs during sample preparation for SEM-EDS characterization.

3.4 TEM-HRETEM and SAED Analysis

The microstructural analysis, particle distribution, and crystalline analysis were performed using TEM, HRTEM, and SAED (JEOL TEM 2100 HRTEM machine). Figure 5a–c, d–f, g–I showed the TEM-HRTEM and SAED pattern of the 1:3, 1:1, and 3:1 volume ratios of Ag NPs, respectively. It can be shown from the TEM images in Fig. 4 that the particles have possessed quasi-spherical microstructure, which is consistent with the morphology obtained via SEM analysis. The formation of this surface structure is crucial for antimicrobial and antioxidant applications of green Ag NPs. Furthermore, green Ag NPs showed black particles dispersed in gray outer regions, which indicates that the abundant phenolic molecules derived from the *Foeniculum vulgare* leaf extract capped the obtained Ag-NPs and prevented agglomeration between the particles of the formed Ag-NPs [26]. The strong capping of the Ag NPs with the leaf extract leads to the formation of smaller average crystalline-sized Ag NPs as can be crosschecked from the XRD analysis. The HRTEM image of each ratio of Ag NPs possessed clear visible crisscross patterns, further confirming the existence of numerous phases in the green Ag NPs [18]. Moreover, the presence of white clear circular spots in the SAED pattern is additional evidence for the formation of crystalline Ag NPs [27]. As presented in Fig. 5c, f, i of the 1:3, 1:1, and 3:1 Ratios of Ag NPs, the SAED pattern nearest to the center of the circle showed clear dots matched to the strong dominant peaks of the (111) miller indices. As far as the center of the circle, small clearly invisible spots were observed, which might present the minor peaks from the XRD data.

3.5 FTIR analysis

In addition to the phytochemical investigation via numerous tests, the possible bioactive ingredient *Foeniculum vulgare* leaf underwent FTIR (PerkinElmer 65) characterization. The analysis was recorded in the wave number range of

4000–400 cm^{-1}. Moreover, this characterization also provides additional hints for the formation of Ag NPs. Figure 6 shows the FTIR spectra of green synthesized Ag (1:1) as representative of the three-volume ratios and leaf of *Foeniculum vulgare*. Absorption bands were located at around 3382, 2929, 2849, 2359, 1620, 1409, 1325, 1249, and 549 cm^{-1}. The hydroxyl groups of phenolic acids and their derivatives could inactivate Ag^{+} ions via chelation. This might be probably due to the high nucleophilicity of their aromatic rings. Since such functional groups release electrons that might convert Ag^{+} to Ag and generate phenolic free radical derivatives. Intern, these generated derivatives reduce other Ag^{+} ions and are oxidized to O-quinones. The quinones coupled with the produced Ag NPs to create a steric barrier around the particles of Ag NPs, preventing them from aggregating and stabilizing their dispersion [28].

The broad absorption intense peaks are found at 3382 and 3402 cm^{-1} of the leaf and green Ag NPs corresponding to the phenolic OH stretching. This very broad O-H stretch band is observed with a C=O peak, which almost certainly indicates that the compound is an aliphatic carboxylic acid.

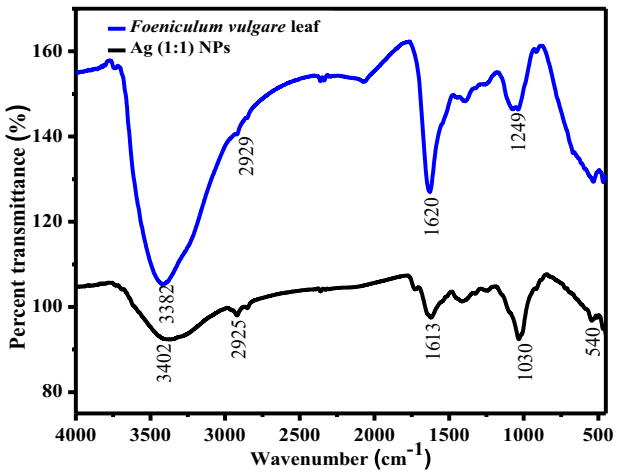

Fig. 6 FTIR spectra of *Foeniculum vulgare* leaf powder and Ag (1:1) NPs

Furthermore, the relatively less intense peaks shown at 2929 and 2849 cm^{-1} correspond to the asymmetric -C-H stretching of $-CH_2$ and $-CH_3$ groups as well as the −C-N group of secondary amines. The presence of such functional groups also conspired via the phytochemical analysis and showed manifestation of the saponin functional groups within the leaf extract. This might also be the absorption band due to the stretching of the C=O vibrations that could emanate from the presence of adsorbed carbon dioxide on the surface of leaf powder and Ag NPs. While the narrower peak of 1613 and 1620 cm^{-1} corresponds to the N-H bending and indicates the presence of secondary amines. Peaks of 1030 and 1249 cm^{-1} refer to the C-O vibration of carbonyl groups of amino acids, peptides, free amino or cysteine groups in proteins found within the leaf extract and also that might bind with the green-formed Ag NPs [29]. The band at 540 cm^{-1} corresponds to the C-H bending mode of vibrations. The observed peak is corresponding to the flavonoids and terpenoid contents of the *Foeniculum vulgare* leaf extract.

3.6 UV-Vis Analysis

The optical properties of synthesized Ag NPs were characterized using the UV-Vis (UV-Vis1800-double beam spectrophotometer, Shimadzu, Japan) spectroscopic technique. As the amount of extract added during the synthesis procedure was altered, each of the volume ratios of Ag NPs showed slight variation in λ_{max}. The variation in light absorption is attributed to the change in conductivity and so optical property (Fig. 7a). The corresponding optical band gap energy was calculated using Tauc's plot method and the calculated value as can be presented in Fig. 7b was found to be 3.3, 3.2 and 3.1 eV for the 1:3, 1:1, and 3:1 volume ratios, respectively. The bad gap energy indirectly fits with the average crystalline size obtained from the XRD data [30]. The current study has been related to the reports of literature. From the band gap energy graph, as the band gap energy decreases, average crystalline size increases, and the optical properties of green Ag NPs are enhanced [31].

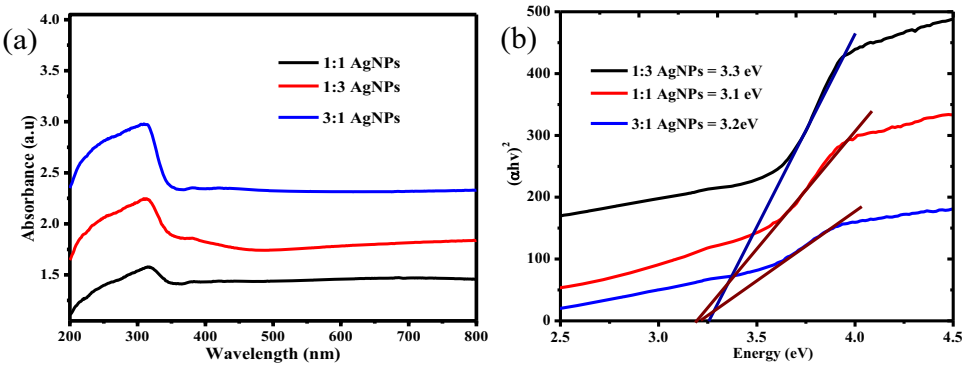

Fig. 7 UV-Vis spectra and band gap energy plot of Ag NPs. **a** UV-Vis spectra of Ag NPs and **b** Tauc's plot

The difference in the intensity and the band position for each ratio is credited to the volume of leaf extract.

3.7 Antimicrobial and antioxidant activity analysis

3.7.1 Antibacterial activity analysis

The antibacterial activity of *Foeniculum vulgare* leaf extract mediated synthesized Ag NPs within the 1:3, 1:1, and 3:1 evaluated via disk diffusion method against *E. coli*, *S.aureus, P.aeruginosa* and *S.pyogen* (Fig. 8 and Table 2). The antibacterial activity test has been carried out within the concentration of 50, 75, and 100 µg/mL. The antibacterial activity of each ratio showed a zone of inhibition between 7.5 and 13.5 mm. From the ratios of Ag NPs, the 1:3 ratios showed the maximum (13.5 mm) zone of inhibition against *S. pyogen (*ATCC19615) as compared to the counterpart ratios at 100 µg/mL dose. This improved activity was obtained due to the enhanced generation of ROS species, which is associated with the excessive volume of leaf extract used during the synthesis procedure [32].

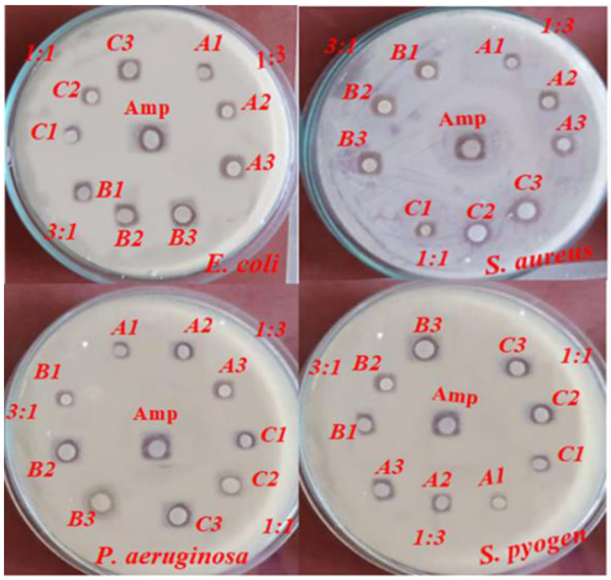

Fig. 8 Antibacterial zone of inhibition by Ag NPs

A minimal (7.5) zone of inhibition was achieved by 3:1 ratios of Ag NPs against *P. aeruginosa (*ATCC27853). This might be ascribed due to the smaller surface area and larger average crystalline size. Furthermore, this might be also contributed by the small generation of ROS species, leading to less effect on the penetration of the Ag^{+} ion towards the cell membrane and then to the death of the bacterial cell membrane. All the volume ratios of Ag NPs are more effective against Gram-positive pathogens, which can be attributed to the absence of an external double membrane. This opportunity enables Ag NPs to easily penetrate the cell membrane of such pathogens slow down the growth of the cell and finally kill the pathogen [26, 33]. The antibacterial activity is found to be dose-dependent. This means as the concentration of green Ag NPs used is higher, the antibacterial activity is also increased linearly as supported in Fig. 8 and Table 2. Excessive accumulation of Ag^{+} in the presence of large amounts of ROS radicals fastens the penetration of the cell of bacteria and this results in the killing of the targeted pathogen [34].

3.8 Antifungal activity analysis

The antifungal activity of the biosynthesized Ag NPs was tested against two fungal strains *Aspergillus niger* (AN) and *Candidca albicans* (CA). The zone of inhibition was measured at different concentrations of 15 mg/mL, 20 mg/mL, and 25 mg/mL for each of the three ratios using ketoconazole as a standard. The value of the zone of

Table 2 Zone of inhibition by Ag NPs against the targeted pathogen supported with the histogram

Ratios of green Ag NPs		Zone of Inhibition (mm)			
		E. coli ATCC25922	*S. aureus* ATCC25923	*P. aeruginosa* ATCC27853	*S. pyogen* ATCC19615
3:1	50 µg/mL	8 ± 0.77	9 ± 0.67	7.5 ± 0. 7	8 ± 0.52
	75 µg/mL	9 ± 0.48	9.5 ± 0. 9	9 ± 0.57	10 ± 0.87
	100 µg/mL	10.5 ± 0. 85	11 ± 0.27	10 ± 0.57	11 ± 0.23
1:3	50 µg/mL	10 ± 0. 80	10.5 ± 0. 89	9 ± 0. 25	11 ± 0. 22
	75 µg/mL	12 ± 0. 35	12 ± 0. 15	12 ± 0. 39	12.5 ± 1. 41
	100 µg/mL	12.5 ± 0. 22	13.5 ± 1. 5	12 ± 0. 85	13.5 ± 0. 95
1:1	50 µg/mL	9 ± 0. 17	9 ± 0. 72	8 ± 0.45	8.5 ± 1. 5
	75 µg/mL	10 ± 0. 85	10 ± 0. 85	10.5 ± 0. 29	10 ± 1. 8
	100 µg/mL	11.5 ± 0. 28	11 ± 1. 25	11 ± 0.81	12.5 ± 0. 49
	Amoxicillin	12.5	14	13	14

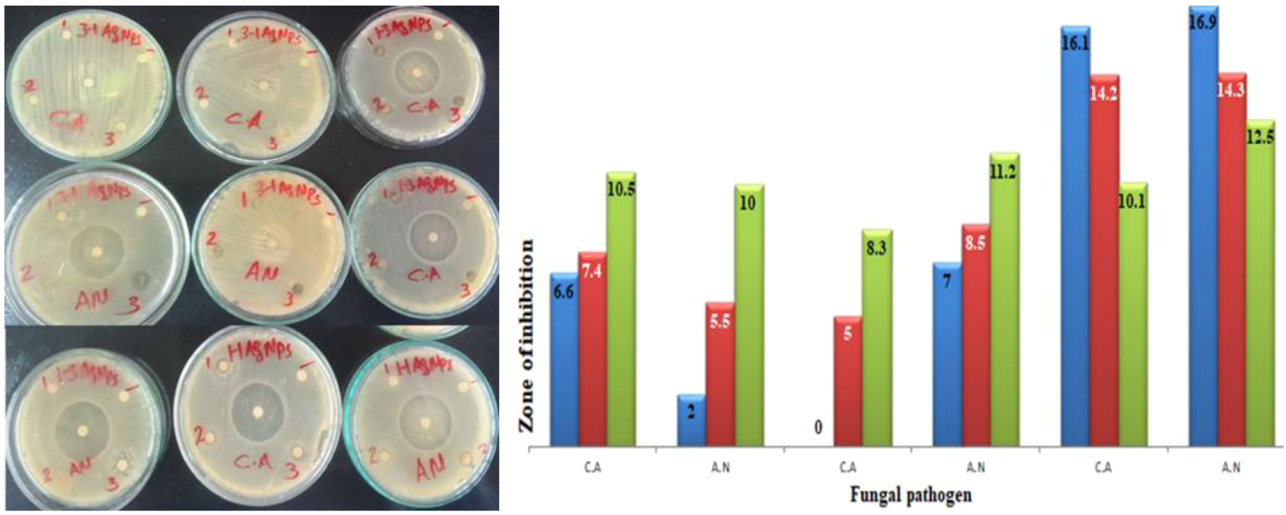

Fig. 9 Antifungal activity of Ag NPs against *Aspergillus niger* and *Candidca albicans*

Table 3 Antifungal zone of inhibition by Ag NPs against *Aspergillus niger and Candida albicans*

Ratio & concentration of Ag NPs		Fungal strains and zone of inhibition in mm ± SD			
		Aspergillus niger		*Candida albicans*	
		Mean ± SD	Ketoconazole	Mean ± SD	Ketoconazole
3:1	15 mg/mL	12.5 ± 3.46	22	10.1 ± 0.59	21
	20 mg/mL	14.3 ± 4.70		14.2 ± 0.25	
	25 mg/mL	16.9 ± 0.3		16.1 ± 0.5	
1:3	15 mg/mL	7 ± 1.5	20	0	15
	20 mg/mL	8.5 ± 0.5		5 ± 0.7	
	25 mg/mL	11.2 ± 0.28		8.3 ± 0.25	
1:1	15 mg/mL	2 ± 0.5	18	6.6 ± 0.85	16
	20 mg/mL	5.5 ± 0.40		7.4 ± 0.76	
	25 mg/mL	10 ± 0.11		10.5 ± 0.26	

inhibition indicates that all the ratios and concentrations of Ag NPs exhibited a varied range of 0–16 mm of antifungal activities against both the tested fungal strains. The formation of inhibition zones around the wells shows fungal sensitivity to antifungal and antibiotic ingredients (Fig. 9) supported by the bar graph. The 1:3 Ag NPs ratios showed strong activity against *Aspergillus niger* with a maximum zone of inhibition of 12.5 ± 3.46, 14.3 ± 4.70, and 16.9 mm at the 15, 20, and 25 mg/mL concentrations, respectively. The second enhanced activity was observed while using the 1:1 Ag NPs ratio with a maximum zone of inhibition of 7, 8.5 ± 0.5, and 11.2 ± 0.28 mm at the concentration of 15, 20, and 25 mg/mL against *Aspergillus niger*, respectively. The 3:1 ratio showed minimal activity comparably, with a zone of inhibition 2 ± 0.5, 5.5 ± 0.40, and 10 ± 0.11 mm at the concentration of 15, 20 and 25 mg/mL against *Aspergillus niger*, respectively [35]. The 1:3 Ag NPs ratio also showed enhanced performance against *Candida albicans* with a maximum zone of inhibition of 10.1 ± 0.59, 14.2 ± 0.25, and 16.1 ± 0.5 mm at the concentrations of 15, 20, and 25 mg/mL, respectively. The second strongest activity showed at a 1:1 ratio with a maximum zone of inhibition of 6.6 ± 0.85, 7.4 ± 0.76, and 10.5 ± 0.26 mm at the concentrations of 15, 20, and 25 mg/mL against *Candida albicans*, respectively. Such like that of *Aspergillus niger*, the 3:1 ratio showed poor performance comparably, with a zone of inhibition of 0, 5, and 8.3 ± 0.26 mm at the concentration of 15, 20, and 25 mg/mL against *Candida albicans*, respectively [36].

The detailed summary of the antifungal activity of Ag (1:3, 1:1, and 3:1) NPs against *Aspergillus niger and Candida albicans* is presented in Table 3.

Among the different ratios of the Ag NPs, the 1: 3 ratios showed better performance of antifungal activity as compared to the remaining two ratios. This might be due to the smaller average crystalline size and large volume of *Foeniculum vulgare* leaf extract [37–40].

Table 4 shows the antioxidant activity of Ag NPs

Con. of Ag NPs (µg/mL)	Control	Ag NPs ratios						Positive control	
		1:1		1:3		3:1		Ascorbic Acid	
	Abs	Abs	%RSA	Abs	%RSA	Abs	%RSA	Abs	%RSA
800	1.1	0.63	42.40	0.80	27.39	0.78	28.94	0.03	97.8
400	1.1	0.77	29.57	0.81	26.48	0.80	27.66	0.04	96.6
200	1.1	0.86	21.75	0.83	24.29	0.84	23.84	0.07	93.34
100	1.1	0.90	17.80	0.85	22.38	0.85	22.57	0.12	88.999
50	1.1	0.92	16.65	0.89	19.11	0.86	22.20	0.14	87.72

Abs Absorbance, *Conc.* Concentration, *%RSA* Percentage radical scavenging activity.

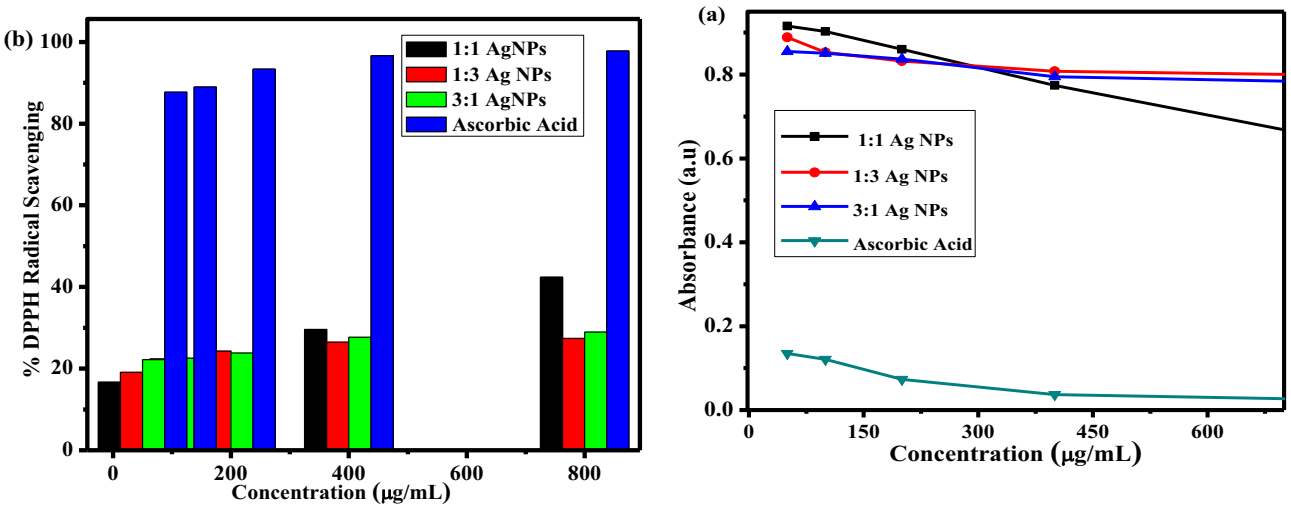

Fig. 10 Concentration of Ag NPs versus absorbance (**a**) and %DPPH versus concentration of Ag NPs (**b**)

3.9 Antioxidant activity analysis

The significant antioxidant potential of *Foeniculum vulgare* leaf-loaded Ag NPs within numerous compositions was evaluated in the presence of DPPH radical scavenging assay at a concentration of 50, 100, 200, 400, and 800 µg/mL in the existence of ascorbic acid as a positive control. The percentage of inhibition observed in all the antioxidant models as the synthesized Ag NPs scavenged free radicals in a concentration-dependent routine up to the given concentration [35, 36]. From the three different volume ratios, 1:3 ratios showed better antioxidant activity as compared to the 1:1 and 3:1 ratios (Table 4). This linearly enhanced activity of the 1:3 ratios is directly related to the presence of a large amount of leaf extract. This is again in line with the excessive accumulation of free ROS species.

The antioxidant activity was found to be in the concentration-dependent to inhibit the free radicals. Interestingly, the higher concentration of each volume ratio produced a higher percentage of antioxidant potential than the lower concentration (Fig. 10 and histogram). The antioxidant potential activities of green Ag NPs align directly with the other antimicrobial applications. The enhanced antioxidant activity of green-formed Ag NPs contributed due to the use of the leaf extract (high generation of ROS species) and the smaller average crystalline size, as well due to the homogenous surface structure. On the other hand, the presence of OH radicals plays a critical role in the lipid peroxidation process [41]. The current findings obtained in the present study divulge that green Ag NPs may scavenge OH radicals and be found to be a promised antioxidant activity. The OH radical scavenging assay was used to find out the antioxidant capacity of green Ag NPs.

In general synthesized Ag NPs obtained in the presence *of Foeniculum vulgare* leaf extract within various compositions, provide strong promising potential applications towards antibacterial activity, antifungal activity, and antioxidant activity too. Table 5 presents a comparison of previous reported work of the literature with the current study.

Table 5 Antimicrobial and antioxidant comparison of previous work with the current study

NPs	Capping agent	Antibacterial activity (mm)	Antifungal activity (mm)	Antioxidant activity (%RSA)	Ref
Ag	*Biarum chaduchrum leaf*	(All in MIC) *S.aureus* = 32, *E. faecalis* = 32, *E. coli* = 64 *P. aeruginosa* = 64	–	–	[42]
Ag	*Saw palmetto seed*	23 against *S.aureus and 28 against E. coli*	–	13.8	[43]
Ag	*Moringa oleifera* leaves	19 *against E. coli*	–	–	[31]
Ag	*Debregeasia Salicifolia*	15 against *E. coli* and 8 against *S.aureus*	–	–	[8]
Ag	*Aloe vera*	9.1 ± 0.100 against *P. aeruginosa*	–	–	[44]
Ag	*Delonix regia* bark	–	–	37.1 ± 0.12	[45]
Ag	*Garcinia Kola* Pulp	–	6 against *Candida tropicalis*	–	[46]
Ag	*Mentha spicata L. (M. spicata)* essential oil	9 against *B. cereus*		40	[43]
Ag	*Foeniculum vulgare* leaf	7.5–15.5	2–16.9	16.65–97.8	Current study

4 Conclusion

Green synthesis of Ag NPs was done in the presence of *Foeniculum vulgare* leaf extract within the 1:3, 1:1, and 3:1 ratios as an effective antimicrobial and antioxidant activity. Characterization was performed using XRD, SEM, TEM, HRETME, SAED, UV-Vis, and FTIR techniques. The synthesized Ag (1:3, 1:1, and 3:1) NPs were crystalline without any phase impurities having quasi-spherical surface morphology in the presence of a major Ag peak. The antimicrobial study proved that *Foeniculum vulgare* leaf-loaded Ag NPs found to be the best candidates for both Gram-negative and Gram-positive pathogens. The efficacy showed that green synthesized Ag NPs showed almost similar performance as the commercially available antibiotics (standard). Antifungal activity of green Ag NPs evaluated against *Aspergillus niger* and *Candida albicans* provides assured activity with a zone of inhibition in between the range of 0–16 mm. In addition, *Foeniculum vulgare* templated synthesized Ag NPs provide surprised antioxidant activity of 97.0%.

Acknowledgements Authors greatly acknowledge Adama Science and Technology University, Ethiopia, and Department of Research Centre, Department of Science, East-West Institute of Technology, Bangalore 560091, India.

Author contributions All authors reviewed the manuscript.

Compliance with ethical standards

Conflict of interest The authors declare no competing interests.

References

1. Zhangabay Z, Berillo D (2023) Antimicrobial and antioxidant activity of AgNPs stabilized with Calendula officinalis flower extract. Results Surf Interfaces 11:100109. https://doi.org/10.1016/j.rsurfi.2023.100109.
2. Zhai Y, Wang B, Han W, Yu B, Ci J, An F (2023) Green synthesis of AgNPs using plant extract and investigation of its anti-human colorectal cancer application. Open Chem 21(1):0–7. https://doi.org/10.1515/chem-2023-0174.
3. Velsankar K, Sudhahar S, Maheshwaran G, Krishna Kumar M (2019) Effect of biosynthesis of ZnO nanoparticles via Cucurbita seed extract on Culex tritaeniorhynchus mosquito larvae with its biological applications. J Photochem Photobiol B: Biol 200:111650. https://doi.org/10.1016/j.jphotobiol.2019.111650.
4. Parmar S, Kaur H, Singh J, Matharu AS, Ramakrishna S, Bechelany M (2022) Recent advances in green synthesis of Ag NPs for extenuating antimicrobial resistance. Nanomaterials 12(7):1115. https://doi.org/10.3390/nano12071115.
5. Velsankar K, Sudhahar S, Parvathy G, Kaliammal R (2020) Effect of cytotoxicity and antibacterial activity of biosynthesis of ZnO hexagonal shaped nanoparticles by Echinochloa frumentacea grains extract as a reducing agent. Mater Chem Phys 239:121976. https://doi.org/10.1016/j.matchemphys.2019.121976.
6. Yugandhar P, Savithramma N (2015) Leaf assisted green synthesis of silver nanoparticles. Nano Biomed Eng 7(2):29–37.
7. Bedlovičová Z, Strapáč I, Baláž M, Salayová A (2020) A brief overview on antioxidant activity determination of silver nanoparticles. Molecules 25(14):3191. https://doi.org/10.3390/molecules25143191.
8. Khan J et al. (2022) Green synthesis of silver nanoparticles (Ag-NPs) Using Debregeasia Salicifolia for biological applications. Materials 16(1):129. https://doi.org/10.3390/ma16010129.
9. Noreen S, Tufail T, Badar Ul Ain H, Awuchi CG (2023) Pharmacological, nutraceutical, functional and therapeutic properties of fennel (Foeniculum vulgare). Int J Food Prop 26(1):915–927. https://doi.org/10.1080/10942912.2023.2192436.
10. Abdelbaky AS et al. (2023) Bio-organic fertilizers promote yield, chemical composition, and antioxidant and antimicrobial activities of essential oil in fennel (Foeniculum vulgare) seeds. Sci Rep. 13(1):13935. https://doi.org/10.1038/s41598-023-40579-7.

11. Salam SGA, Rashed MM, Ibrahim NA, Rahim EAA, Aly TAA, AL-Farga A (2023) Phytochemical screening and in-vitro biological properties of unprocessed and household processed fenugreek (Trigonella foenum-graecum Linn.) seeds and leaves. Sci Rep. 13(1):1–13. https://doi.org/10.1038/s41598-023-31888-y.
12. Beyazen A, Dessalegn E, Mamo W (2017) Phytochemical screening and biological activities of leaf of Foeniculum vulgare (Ensilal). World J Agric Sci 13(1):1–10. https://doi.org/10.5829/idosi.wjas.2017.01.10.
13. Barakat H et al. (2022) Phenolics and volatile compounds of Fennel (Foeniculum vulgare) seeds and their sprouts prevent oxidative DNA damage and ameliorates CCl4-induced hepatotoxicity and oxidative stress in rats. Antioxidants, 11, 12, https://doi.org/10.3390/antiox11122318.
14. Barwant M et al. (2022) Eco-friendly synthesis and characterizations of Ag/AgO/Ag2O nanoparticles using leaf extracts of Solanum elaeagnifolium for antioxidant, anticancer, and DNA cleavage activities. Chem Pap 76(7):4309–4321. https://doi.org/10.1007/s11696-022-02178-0.
15. Bano I, Deora GS (2020) Preliminary phytochemical screening and gc-ms analysis for identification of bioactive compounds from Abutilon Fruticosum Guill and Perr. a rare and endemic plant of Indian Thar desert. Int J Pharm Sci Res 11(6):2671–2679. https://doi.org/10.13040/IJPSR.0975-8232.11(6).2671-79.
16. Tilahun E, Yilkal B, Sintayehu D, Murthy HCA, Shegaw M (2022) Synthesis of ZnO nanoparticles mediated by natural products of Acanthus sennii leaf extract for electrochemical sensing and photocatalytic applications: a comparative study of volume ratios. Chem Pap, 0123456789. https://doi.org/10.1007/s11696-022-02301-1.
17. Dejen KD et al. (2023) Green synthesis and characterisation of silver nanoparticles from leaf and bark extract of Croton macrostachyus for antibacterial activity. Mater Technol, 38, 1. https://doi.org/10.1080/10667857.2022.2164647.
18. Abdel-Aty AM, Barakat AZ, Bassuiny RI, Mohamed SA (2023) Statistical optimization, characterization, antioxidant and antibacterial properties of silver nanoparticle biosynthesized by saw palmetto seed phenolic extract. Sci Rep. 13(1):15605. https://doi.org/10.1038/s41598-023-42675-0.
19. Suresh P, Doss A, Praveen Pole RP, Devika M (2023) Green synthesis, characterization and antioxidant activity of bimetallic (Ag-ZnO) nanoparticles using Capparis zeylanica leaf extract. Biomass Convers Biorefin, 0123456789. https://doi.org/10.1007/s13399-023-03743-7.
20. Verma R, Rani L (2023) Phytochemical and antimicrobial potential of methanolic leaf extracts of Acacia catechu and Lagerstroemia speciosa against Escherichia coli O157:H7. Available: https://www.researchgate.net/publication/375558203
21. Shaikh JR, Patil M (2020) Qualitative tests for preliminary phytochemical screening: An overview. Int J Chem Stud 8(2):603–608. https://doi.org/10.22271/chemi.2020.v8.i2i.8834.
22. Giri AK et al. (2022) Green synthesis and characterization of silver nanoparticles using Eugenia roxburghii DC. extract and activity against biofilm-producing bacteria. Sci Rep. 12(1):8383. https://doi.org/10.1038/s41598-022-12484-y.
23. Yasmin S et al. (2020) Green synthesis, characterization and photocatalytic applications of silver nanoparticles using Diospyros lotus. Green Process Synth 9(1):87–96. https://doi.org/10.1515/gps-2020-0010.
24. Al-Namil DS, El Khoury E, Patra D (2019) Solid-state green synthesis of Ag NPs: Higher temperature harvests larger Ag NPs but smaller size has better catalytic reduction reaction. Sci Rep. 9(1):15212. https://doi.org/10.1038/s41598-019-51693-w.
25. Siddiqi KS, Husen A, Rao RAK (2018) A review on biosynthesis of silver nanoparticles and their biocidal properties. J Nanobiotechnol, 2018, https://doi.org/10.1186/s12951-018-0334-5.
26. Zhang XF, Liu ZG, Shen W, Gurunathan S (2016) Silver nanoparticles: Synthesis, characterization, properties, applications, and therapeutic approaches. Int J Mol Sci, 17, 9, https://doi.org/10.3390/ijms17091534.
27. Shu M et al. (2020) Biosynthesis and antibacterial activity of silver nanoparticles using yeast extract as reducing and capping agents. Nanoscale Res Lett, 15, 1 https://doi.org/10.1186/s11671-019-3244-z.
28. Vanlalveni C, Lallianrawna S, Biswas A, Selvaraj M, Changmai B, Rokhum SL (2021) Green synthesis of silver nanoparticles using plant extracts and their antimicrobial activities: a review of recent literature. RSC Adv 11(5):2804–2837. https://doi.org/10.1039/d0ra09941d.
29. Qamer S et al. Systematic review on biosynthesis of silver nanoparticles and antibacterial activities: Application and theoretical perspectives Molecules, 26, 16, 2021, https://doi.org/10.3390/molecules26165057.
30. Gevorgyan S, Schubert R, Falke S, Lorenzen K, Trchounian K, Betzel C (2022) Structural characterization and antibacterial activity of silver nanoparticles synthesized using a low-molecular-weight Royal Jelly extract. Sci Rep. 12(no. 1):1–12. https://doi.org/10.1038/s41598-022-17929-y.
31. Asif M, Yasmin R, Asif R, Ambreen A, Mustafa M, Umbreen S (2022) Green synthesis of silver nanoparticles (AgNPs), structural characterization, and their antibacterial potential. Dose-Response 20(1):1–11. https://doi.org/10.1177/15593258221088709.
32. Hano C, Abbasi BH (2022) Plant-based green synthesis of nanoparticles: Production, characterization and applications. Biomolecules 12(1):1–9. https://doi.org/10.3390/biom12010031.
33. Bruna T, Maldonado-Bravo F, Jara P, Caro N (2021) Silver nanoparticles and their antibacterial applications. Int J Mol Sci 22(13):7202. https://doi.org/10.3390/ijms22137202.
34. Velsankar K, Preethi R, Ram PSJ, Ramesh M, Sudhahar S (2020) Evaluations of biosynthesized Ag nanoparticles via Allium Sativum flower extract in biological applications. Appl Nanosci 10(9):3675–3691. https://doi.org/10.1007/s13204-020-01463-2.
35. Hashem AH et al. (2022) Antifungal activity of biosynthesized silver nanoparticles (AgNPs) against Aspergilli causing Aspergillosis: Ultrastructure study. J Funct Biomater, 13, 4, https://doi.org/10.3390/jfb13040242.
36. Wang D, Xue B, Wang L, Zhang Y, Liu L, Zhou Y (2021) Fungus-mediated green synthesis of nano-silver using Aspergillus sydowii and its antifungal/antiproliferative activities. Sci Rep. 11(1):1–9. https://doi.org/10.1038/s41598-021-89854-5.
37. Shi H et al. (2023) Antifungal activity and mechanisms of AgNPs and their combination with azoxystrobin against Magnaporthe oryzae. Environ Sci: Nano 10(9):2412–2426. https://doi.org/10.1039/d3en00168g.
38. Khan M, Khan AU, Bogdanchikova N, Garibo D (2021) solanacearum and Fusarium oxysporum. Molecules 26(no. 9):2462. https://doi.org/10.3390/molecules26092462.
39. Sharifi-Rad M, Pohl P (2020) Synthesis of biogenic silver nanoparticles (Agcl-nps) using a pulicaria vulgaris gaertn. aerial part extract and their application as antibacterial, antifungal and antioxidant agents. Nanomaterials 10(4):1–17. https://doi.org/10.3390/nano10040638.
40. Velsankar K, Aswin Kumara RM, Preethi R, Muthulakshmi V, Sudhahar S (2020) Green synthesis of CuO nanoparticles via Allium sativum extract and its characterizations on antimicrobial, antioxidant, antilarvicidal activities. J Environ Chem Eng 8(5):104123. https://doi.org/10.1016/j.jece.2020.104123.
41. Velsankar K, Parvathy G, Mohandoss S, Krishna Kumar M, Sudhahar S (2022) Celosia argentea leaf extract-mediated green synthesized iron oxide nanoparticles for bio-applications. J Nanostruct Chem 12(4):625–640. https://doi.org/10.1007/s40097-021-00434-5.

42. Vakili S et al. (2022) Green synthesis, characterization and antibacterial activity of silver nanoparticles by Biarum chaduchrum leaf extract. Appl Phys A: Mater Sci Process 128(3):1–6. https://doi.org/10.1007/s00339-022-05384-5.
43. Moosavy MH, de la Guardia M, Mokhtarzadeh A, Khatibi SA, Hosseinzadeh N, Hajipour N (2023) Green synthesis, characterization, and biological evaluation of gold and silver nanoparticles using Mentha spicata essential oil. Sci Rep. 13(1):1–15. https://doi.org/10.1038/s41598-023-33632-y.
44. Alwhibi MS, Soliman DA, Awad MA, Alangery AB, Al Dehaish H, Alwasel YA (2021) Green synthesis of silver nanoparticles: Characterization and its potential biomedical applications. Green Process Synth 10(1):412–420. https://doi.org/10.1515/gps-2021-0039.
45. Bala A, Rani G (2023) Green synthesis of AgNPs using Delonix regia bark for potential catalytic and antioxidant applications. Microsc Res Tech 86(8):911–922. https://doi.org/10.1002/jemt.24310.
46. Akintelu SA, Olugbeko SC, Folorunso AS (2022) Green synthesis, characterization, and antifungal activity of synthesized silver nanoparticles (AgNPS) from Garcinia Kola pulp extract. BioNanoScience 12(1):105–115. https://doi.org/10.1007/s12668-021-00925-3.